J Supercond Nov Magn (2018) 31:233–239
DOI 10.1007/s10948-017-4196-0

ORIGINAL PAPER

Structural, Electronic, Magnetic, and Optical Properties of Half-Heusler Alloys RuMnZ (Z = P, As): a First-Principle Study

Nasir Mehmood[1] · **Rashid Ahmad**[1]

Received: 6 February 2017 / Accepted: 12 June 2017 / Published online: 22 June 2017

Abstract Half-Heusler alloys RuMnZ (Z = P, As) are studied in the framework of Density Functional Theory (DFT). Structural, electronic, magnetic, and optical properties are calculated and analyzed using the WIEN2k simulation code. All the calculations are done using the full potential linearized augmented plane wave (FP-LAPW) method. Equilibrium lattice parameters are found to be in the range 5.5–5.6 Å. Band gaps of the compounds and density of states (DoS) analysis reveal that the minority spin-down states are semi-conducting while the majority spin-up states are conducting confirming the half-metallic nature of the compounds. Hence, at Fermi level, states are 100% polarized. The value of the total magnetic moment is found to be 2, i.e., $M_{Tot} = 2\mu_B$. Several optical properties, including dielectric function, reflectivity, refractive index, conductivity, and absorption coefficient are calculated as well. It is revealed from the imaginary part of the dielectric function that the compounds are optically metallic.

Keywords Half-Heusler alloys · Half-metallic compounds · Optical properties · Ferromagnetic materials

1 Introduction

In the seminal work of de Groot et al., two ternary half-Heusler compounds namely NiMnSb and PtMnSb were investigated, and they predicted their half-metallic nature [1, 2]. Later, an important class of materials chromium dioxide CrO_2 was shown to be half-metallic ferromagnetic by Shwarz [3]. Matar et al. have calculated its electronic and magnetic properties under pressure [4]. Full and half-Heusler alloys are two major types of Heusler alloys. They have four fcc lattices and usually crystallize in $L2_1$ and $C1_b$ structures correspondingly. Ternary form of half-Heusler alloys is XYZ and of full-Heusler alloys X_2YZ. In these formulas, X and Y represent high and low valent transition metals, respectively, and Z denotes sp electron atom. There has been recently an increasing interest in calculating different properties and aspects of half-Heusler materials. Some of the very recent works include simulation study of various properties such as structural, electronic, and magnetic properties of YMnSb and YCrSb in [5]. Structural and electronic properties of half-Heusler alloys PtXBi (with X = Mn, Fe, Co and Ni) calculated from first principles in [6]. Optical properties of RbSrZ where Z representing C, Si, Ge are examined in [7]. Thermoelectric properties of half-Heusler alloys are calculated in [8]. Half-Heusler alloys with the direct band gap of 1.7 eV for solar cell applications are analyzed in [9].

Half-metallic materials, have the minority spin channel (usually spin-down) of semiconducting nature while the majority spin channel (usually spin-up) of metallic behavior. The occurrence of such a hybrid behavior at the Fermi level produces full (100%) spin polarization. These materials then develop fully spin-polarized current, which helps to maximize the efficiency of magneto-electronic devices. A wide variety of materials, including transition metal pnictides and metal-chalcogenides [10, 11], different types of perovskites [12, 13], oxides [14, 15], magnetic semiconductors [16, 17], and all types of Heusler alloys [18, 19] have shown to be half-metals. Such magnetic materials have found important applications in the field of spintronics [20–22].

✉ Nasir Mehmood
nasir_ph@yahoo.com

[1] Department of Physics, Kohat University of Science and Technology, Kohat 26000, Khyber Pakhtunkhwa, Pakistan

In this work, we analyze structural, electronic, magnetic, and optical properties of the half-Heusler alloys RuMnZ (P, As). The RuMnAs alloy is already experimentally synthesized [23]. The computational study of 378 XYZ compounds, including RuMnZ (Z = P, As) is done in [24]. They are half-metallic half-Heusler alloys, which are not investigated theoretically. We, therefore, present a comprehensive study of their properties.

The rest of this manuscript is organized as follows. In the Section 2 we have described the computational setup, values of different parameters and methods used in this work. The next Section 3 includes the results obtained, and the discussion on all properties examined in the work. Summary and conclusions are presented in the last Section 4.

2 Simulation Setup

We have used the WIEN2k code [25] to simulate the alloys. Their different properties are determined using the FP-LAPW method [26]. Furthermore, to examine the exchange-correlation (EC) effects Perdew–Burke–Ernzerhof (PBE) [27, 28] exchange-correlation functional (ECF) in the generalized gradient approximation (GGA) approach is used. We have optimized the geometry and electronic structure by the FP-LAPW method using the spin-polarized Density Functional Theory (SDFT). To determine densities of majority spin-up (↑) and minority spin-down (↓) states, the Kohn–Sham system of equations are solved self-consistently [29, 30]. The core and valance-states-energy-gap is chosen to be −6 Ry. The spherical harmonic functions with cut-off (l-max = 10) inside the muffin-tin-spheres are used. Furthermore, the RK max is 2.5, KPoints are taken to be 1000 and G-max is 12.

Ternary half-Heusler alloys are inter-metallic alloys in the chemical composition of XYZ where X and Y represent different transition metals and Z is an element from the main group. The space group is F43m (No. 216) and X atoms are located at Wyckoff positions in the non-equivalent 4a (1/4,1/4,1/4) whereas the Y and Z atoms are positioned at the 4b (1/2,1/2,1/2) and 4d (0,0,0), respectively, as shown in the Fig. 1. In the Table 1, we have listed five configurations of atomic arrangements. Type 4 is the only configuration where the alloys show the half-metallic behavior.

3 Results and Discussions

This section is dedicated to the detailed explanations of properties of half-Heusler alloys RuMnZ (Z = P, As). We have, first of all, checked the stability of the crystal structure of the alloys. The variation of total energies of RuMnZ (Z = P, As) with respect to volume is shown in the Fig. 2.

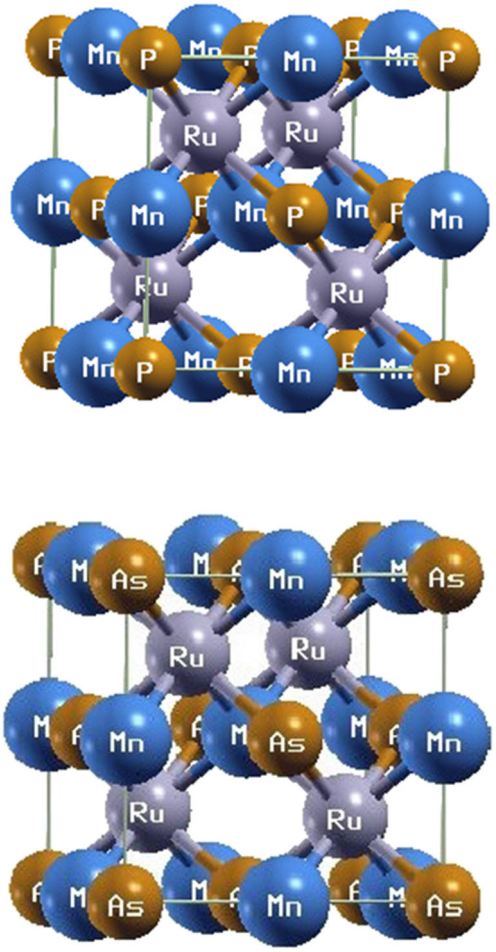

Fig. 1 Crystal structure of half-Heusler alloys **a** RuMnP **b** RuMnAs

It is evident that the equilibrium value of unit cell volume increases as we move from P to As. The equilibrium lattice constants of both compounds are calculated and listed in the Table 2. We can see that the values of lattice constant increases with the increase in atomic number Z. This increase is due to the larger radius of Phosphorus (P) as compared to Arsenic (As). These calculations are performed with spin-polarization included.

Table 1 Various configurations of atomic arrangements in half-Heusler structure

X	Y	Z	HM	
Type 1	(0, 0, 0)	(1/2, 1/2, 1/2)	(1/4, 1/4, 1/4)	No
Type 2	(1/2, 1/2, 1/2)	(0, 0, 0)	(1/4, 1/4, 1/4)	No
Type 3	(1/4, 1/4, 1/4)	(0, 0, 0)	(1/2, 1/2, 1/2)	No
Type 4	(1/4, 1/4, 1/4)	(1/2, 1/2, 1/2)	(0, 0, 0)	Yes
Type 5	(1/2, 1/2, 1/2)	(1/4, 1/4, 1/4)	(0, 0, 0)	No

Only type 4 shows the half-metallic nature

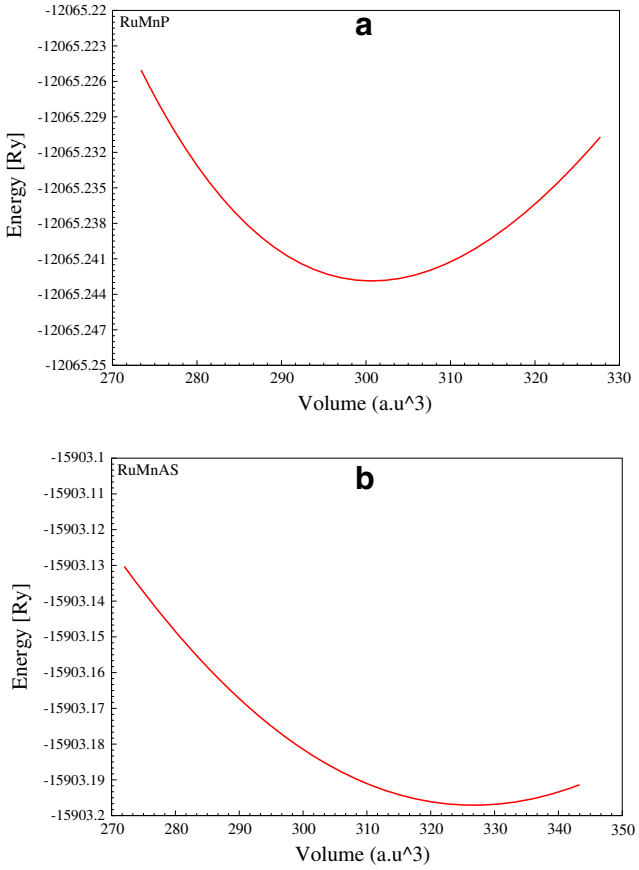

Fig. 2 Total energy variation with respect to volume for **a** RuMnP and **b** RuMnAs

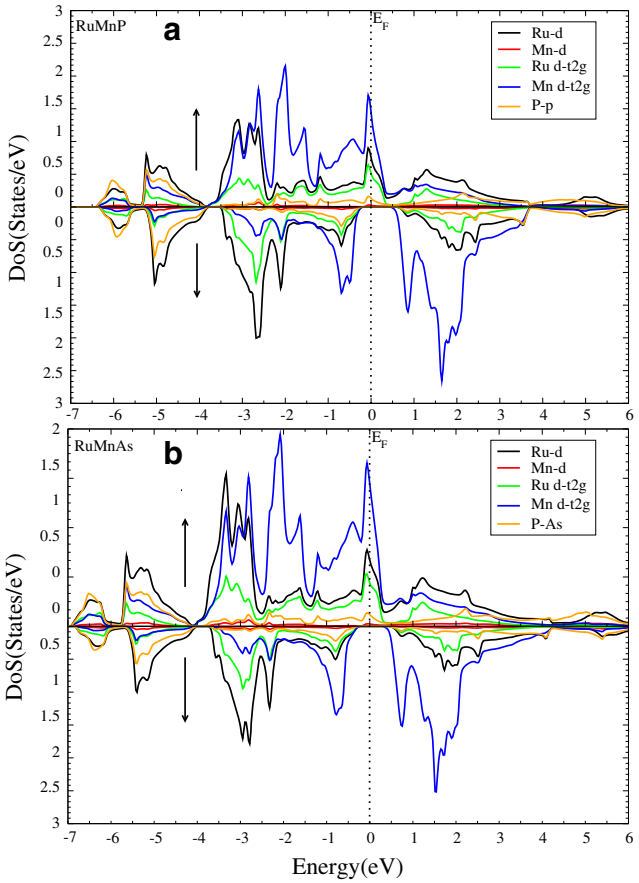

Fig. 3 The calculated total DoS's for the **a** RuMnP and **b** RuMnAs compounds. DoS-positive values represent majority spin electrons and negative-value minority electrons. The zero value of energy corresponds to Fermi Level

3.1 Electronic Properties

The electronic properties of materials are essential to reveal the half-metallic nature of the materials. Density of States (DoS) for both alloys are shown in the Fig. 3. We can see that the major contributions come from Z-p and the d states of Ruthenium (Ru) and Manganese (Mn).

We have also calculated the band structure to determine their half-metallicity using GGA approximation. In spin-down configuration, Z-p dominated the conduction band and has produced the band gap, while, in spin-up configuration Z-p state cross over by the Fermi level and produce the metallic nature in this channel and hence compounds becomes half-metallic.

Table 2 Lattice constants $a_0(\AA)$ of the half-Heusler alloys RuMnZ (Z = P, As)

Alloy	$a_0(\AA)$ (this work)	$a_0(\AA)$ (other work)
RuMnP	5.50	5.59 [24]
RuMnAs	5.56	5.76 [24]

The band structure of minority and majority spin channels can also show that if materials are metallic or semiconducting in the particular channel. The spin-polarized band structures of RuMnZ (Z = P, As) are shown in the Fig. 4 where the panels at the left are the majority channels (spin-up (↑)) and right panels are the minority channels (spin-down (↓)). It is evident that in the majority channel, there is no band gap, which shows the metallic nature of the compounds in this channel and in the minority channel, there is a band gap which reveals the semiconducting nature of the compounds in the channel. There are indirect small band gaps of 0.54 and 0.58 eV, respectively, where the maximum of the valence band occurs at the L-point and conduction band minimum is at the X-point; therefore, the compounds RuMnZ (Z = P, As) show half-metallic behavior (Table 3).

The band gaps completely (100%) spin polarize both the alloys at Fermi energy E_F, resulting in the half-metallic nature. Additionally, the energy gaps are found to be responsive to the lattice parameters.

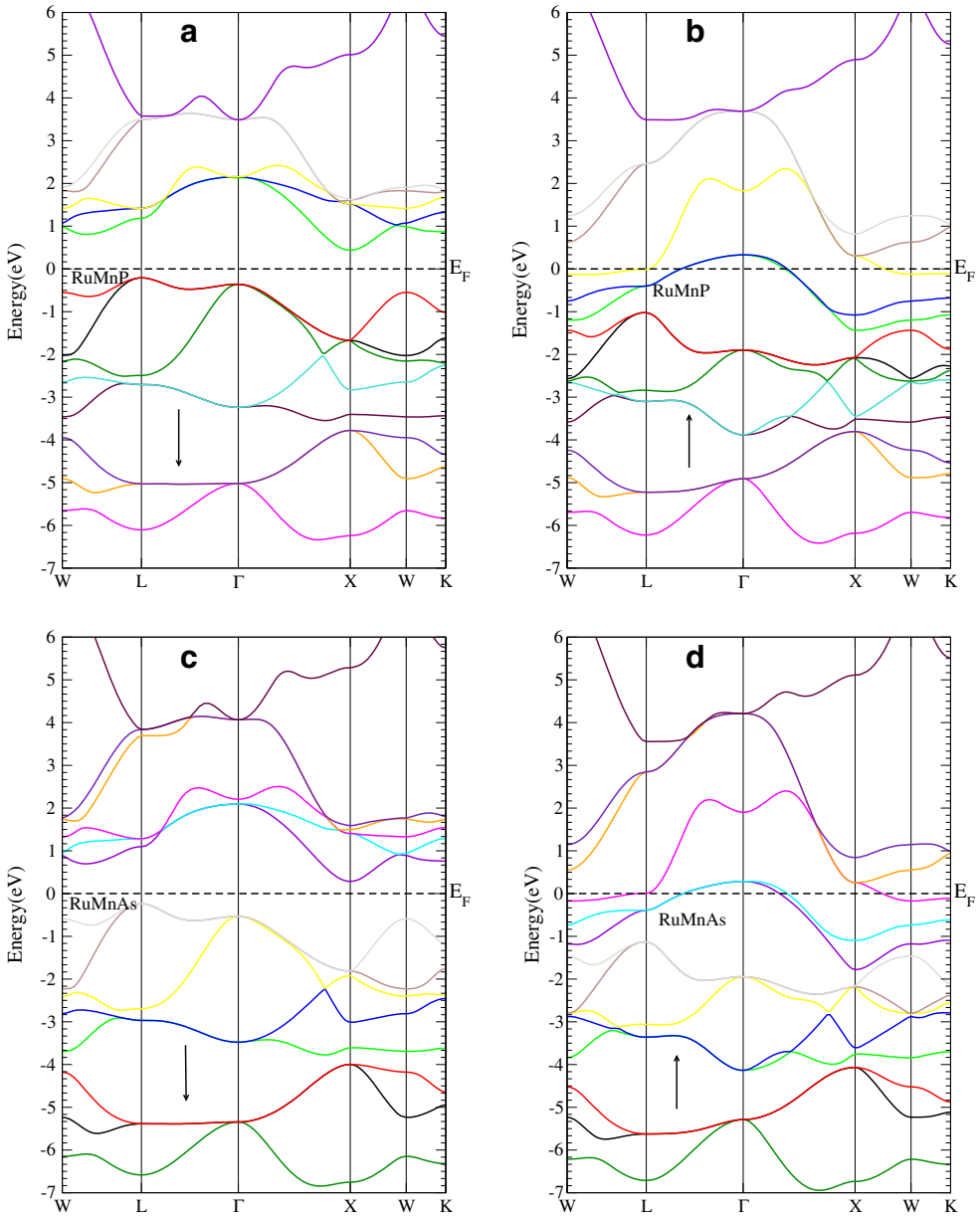

Fig. 4 At the equilibrium lattice parameter, the band structure of RuMnZ (Z = P, As) is shown. The *dashed horizontal line* at zero eV (E_F) represents the Fermi Level

It can be seen from the Fig. 3 that the number of states occupied at the specific energy level are determined by the DoS. The partial DoS are depicted for both the alloys in the Fig. 3. Large spin splitting comes from Mn ($d - t_{2g}$) states, and the contribution from Ru ($d - t_{2g}$) states is relatively small. However, P and As atoms contribution is very small.

Table 3 Band gaps of RuMnZ (Z = P, As)

Alloy	E_g^{W-W}	E_g^{L-L}	$E_g^{\Gamma-\Gamma}$	E_g^{X-X}	E_g^{k-k}	E_g^{L-X}
RuMnP	1.49	1.37	2.60	2.00	1.86	0.54
RuMnAs	1.37	1.32	2.33	2.06	0.78	0.58

3.2 Magnetic Properties

Slater-Pauling 18 electron-rule $M_{Tot} = 18 - Z_{Tot}$ is the basis for magnetic behavior in half-Heusler alloys reported by Kubler for the first time. According to the model [31, 32] presented by Galanakis the spin-magnetic moment of half-Heusler alloys is equal to the difference of occupied bands in up and down spin states. Such compounds have the C1b structure where three atoms are located per unit cell and follow the Slater-Pauling rule. In the above relation, M_{Tot} and Z_{Tot} mean spin-magnetic moment and a total number of valence electrons respectively, where the number of occupied states is 18 in the spin bands. In this work for ternary 1:1:1 half-Heusler compounds the calculated M_{Tot}

Table 4 The magnetic moments in terms of (μ_B), are given where M_Z represents P and As atoms, and the unit cell total magnetic moment is given M_{Tot}. M_{Inst} is interstitial magnetic moments for RuMnZ (Z = P, As)

Alloy	M_{Tot} (this work)	M_{Tot} (other work)	M_{Ru}	M_{Mn}	M_Z	M_{Inst}
RuMnP	2.00	2.00 [24]	−0.16	2.22	−0.02	0.034
RuMnAs	2.00	2.00 [24]	−0.27	2.34	−0.03	−0.007

is $2\mu_B$. We have shown in the Table 4 the total magnetic moment, and contributions from atomic resolved and interstitial magnetic moments for RuMnZ (Z = P, As). The major contributions to the total magnetic moments come from Mn atoms.

3.3 Optical Properties

The optical properties of materials are determined by dielectric function $\epsilon(\omega)$. In specific, linear response of a system to an external electromagnetic field is given by it. The mathematical form is given by the Ehrenreich and Cohen's equation

$$\epsilon(\omega) = \epsilon_1(\omega) + i\epsilon_2(\omega). \quad (1)$$

The imaginary part $\epsilon_2(\omega)$ is shown in the following formula

$$\epsilon_2(\omega) = \frac{4\pi e^2}{m^2\omega} \int d^k \Sigma_{n,n'} |< kn \mid p \mid kn' >|^2 \times f_{kn}(1 - f_{k'n'})\delta(E_{kn} - E_{kn'} - \hbar\omega). \quad (2)$$

The Kramers–Kronig Transformation (KKT) is used for the value of the real part of $\epsilon(\omega)$ i.e. $\epsilon_1(\omega)$

$$\epsilon_1(\omega) = 1 + \frac{2}{\pi} M \int_0^\infty \frac{\omega' \epsilon_2(\omega')}{\omega'^2 - \omega^2} d\omega' \quad (3)$$

An important optical parameter is refractive index $n(\omega)$ which is obtained in terms of the complex dielectric function as given in [33, 34]

$$n(\omega) = \frac{1}{\sqrt{2}} \left(\epsilon_1 + \left(\epsilon_1^2 + \epsilon_2^2 \right)^{\frac{1}{2}} \right)^{\frac{1}{2}} \quad (4)$$

Another optical property known as reflectivity $R(\omega)$ of RuMnZ (Z = P, As) is derived immediately from $\epsilon_1(\omega)$ and $\epsilon_2(\omega)$.

Figure 5a, g shows the real and imaginary parts of the total dielectric function of RuMnP and RuMnAs, respectively. Analyzing the band structure and DoS, it is realized that the peaks mainly result from transitions in spin-down channel. The calculated values of real and imaginary parts $\epsilon(\omega)$ at (0eV) for both compounds are almost the same.

The $\epsilon_2\uparrow(\omega)$ and $\epsilon_2\downarrow(\omega)$ are plotted in the Fig. 5b, h. The peaks are observed in the small energy range and it vanishes at about 11 eV.

The high value of imaginary part of the dielectric function $\epsilon\uparrow(\omega)$ reveals the metallic nature of the compounds.

Refractive index of a material is an important parameter for photoelectric applications. Refractive indices of RuMnZ (Z = P, As) are shown in the Fig. 5c, i, respectively. It is clear that refractive indices have several peaks in the infrared region and gradually decrease in the visible region. These

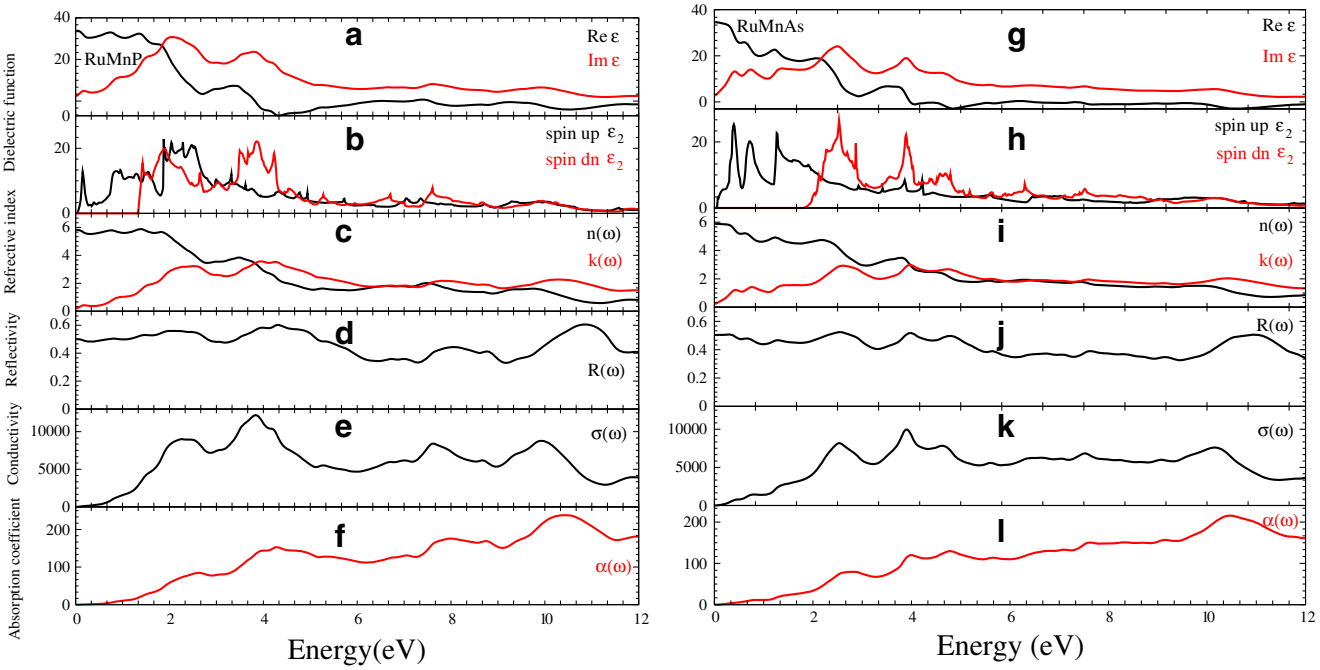

Fig. 5 Optical properties of RuMnZ (Z = P, As)

peaks arise from the interband transition between the topmost valence band and the lowermost conduction band. This peaks in the infrared region show that the refractive index has a nonlinear behavior.

The imaginary parts $n(k)$ which is also called extension coefficient is also shown in the Fig. 5c, i for RuMnP and RuMnAs, respectively. It also have peaks in the infrared region resulting from interband transitions. Both real and imaginary parts start at opposite ends, i.e, their maximum and minimum values and meet at about 3 eV and afterwards show roughly same behavior.

For optical spectra shown in Fig. 5d, j, we see the somehow stable reflectivity at all energies up to 12 eV.

It is also observed that the real part, i.e., ϵ_1 of the dielectric function becomes negative for energetic photons; hence, reflectivity peaks are obtained, showing again the metallic nature of the compounds, i.e., energy range of these materials where they become more reflective to the incident photons.

Optical conductivity in Fig. 5e, k characterizes the metallic nature of the materials.

The absorption coefficient is shown in the Fig. 5f, l. The peaks are resulting from peaks in the ϵ_2. In the infrared region, spectrum shows increase in the width which may be due to transitions between closely separated energy levels.

4 Conclusions

We have investigated the half-Heusler alloys RuMnZ (Z = P, As) using WIEN2K code and PBE-GGA in the framework of DFT for structural, electronic, magnetic, and optical properties. The values obtained of equilibrium lattice constants show that compounds are structurally stable.

Half-metallic properties are observed so that, both the compounds have the metallic nature in spin-up and semiconducting in spin-down with the indirect small band gap.

For magnetic properties, we observed that spin magnetic moment is approximately equal to 2, i.e., $M_{Tot} \approx 2u_B$.

The real and imaginary parts of dielectric function, refractive index, and the real part of reflectivity, optical conductivity, and absorption coefficient are calculated whereas imaginary part of dielectric function ϵ_2 shows that the alloys are optically metallic.

References

1. de Groot, R.A., Mueller, F.M., Engen, P.G.V., Buschow, K.H.J.: New class of materials: half-metallic ferromagnets. Phys. Rev. Lett. **50**, 2024 (1983)
2. de Groot, R.A., Mueller, F.M., Engen, P.G.V., Buschow, K.H.J.: Recent developments in half-metallic magnetism. J. Magn. Magn. Mater. **54**, 1377 (1986)
3. Shwarz, K.: CrO_2 predicted as a half-metallic ferromagnet. J. Phys. F Metal Phys. **16**, L211 (1986)
4. Martar, S., Demazeau, G., Sticht, J., Eyert, V., Kübler, J.: Etude de la structure électronique et magnétique de CrO_2. J. Phys. I France **2**, 315 (1992)
5. Sattar, M.A., Rashid, M., Hashmi, M.R., Ahmad, S.A., Imran, M., Hussain, F.: Etude de la structure électronique et magnétique de CrO_2. J. Phys. I France **2**, 315 (1992)
6. Huang, W., Wang, X., Chen, X., Lu, W., Damewood, L., Fong, C.Y.: Structural and electronic properties of half-Heusler alloys PtXBi (with X = Mn, Fe, Co, Ni) calculated from first principles. J. Magn. Magn. Mater. **377**, 252 (2015)
7. Ahmad, M., Naeemullah, G., Murtaza, R., Khenata, S.B., Omran, A.: Bouhemadou, structural, elastic, electronic, magnetic and optical properties of RbSrX(C, Si, Ge) half-Heusler compounds. J. Magn. Magn. Mater. **377**, 204 (2015)
8. Sattar, M.A., Rashid, M., Hashmi, M.R., Ahmad, S.A., Imran, M., Hussain, F.: Full-scale computation for all the thermoelectric property parameters of half-Heusler compounds. Sci. Rep. **6**, 22778 (2016)
9. Sattar, M.A., Rashid, M., Hashmi, M.R., Ahmad, S.A., Imran, M., Hussain, F.: Half-heusler compounds with a 1 eV (1.7 eV) direct band gap, lattice-matched to GaAs (Si), for solar cell application: A first-principles study. Phys. Status Solidi B **253**, 253 (2016)
10. Galanakis, I., Mavropoulos, P.: Zinc-blende compounds of transition elements with N, P, As, Sb, S, Se, and Te as half-metallic systems. Phys. Rev. B **67**, 104417(1) (2003)
11. Galanakis, I., Mavropoulos, P.: First-principles study of half-metallic ferromagnetism in $Zn_{1-x}CrSe$. J. Magn. Magn. Mater. **321**, 198 (2009)
12. Kobayashi, K.I., Kimura, T., Sawada, H., Terakura, K., Tokura, Y.: Room-temperature magnetoresistance in an oxide material with an ordered double-perovskite structure. Nature **95**, 677 (1998)
13. Zhu, Z.H., Yan, X.H.: Half-metallic properties of perovskite $BaCro_3$ and $BaCr_{0.5}Ti_{0.5}O_3$ superlattice: LSDA+u calculations. J. Appl. Phys. **106**, 023713(1) (2009)
14. Soeya, S., Hayakawa, J., Takahashi, H., Ito, K., Yamamoto, C., Kida, A., Asano, H., Matsui, M.: Development of half-metallic ultrathin Fe_3O_4 films for spin-transport devices. Appl. Phys. Lett. **95**, 677 (1998)
15. Dho, J., Ki, S., Gubkin, A.F., Park, J.M.S., Sherstobitova, E.A.: A neutron diffraction study of half-metallic ferromagnet nanorods. J. Phys. Chem. Solids **150**, 86 (2010)
16. Kronik, L., Jain, M., Chelikowsky, J.R.: Electronic structure and spin polarization of $Mn_{,x}$ $Ga_{1-x}N$. Phys. Rev B **66**, 041203 (2002)
17. Noor, N.A., Ali, S., Shaukat, A.: First principles study of half-metallic ferromagnetism in Cr-doped CdTe. J. Phys. Chem. Solids **72**, 841 (2011)
18. Nourmohammadi, A., Abolhasani, M.R.: First-principle study of full Heusler using {PBE0} hybrid functional. Solid State Commun. **150**, 1501 (2010)
19. Wang, W.Z., Wei, X.P.: Half-metallic antiferromagnetic in Mn_2ZnCa. Comput. Mater. Sci. **50**, 2253 (2011)
20. Nourmohammadi, A., Abolhasani, M.R.: Tunneling between ferromagnetic films. Phys. Lett. A **54**, 225 (1975)
21. Ohno, H.: Making nonmagnetic semiconductors ferromagnetic. Science **281**, 951 (1998)
22. Jimbo, M., Hirano, S., Meguro, K., Tsunashima, S., Uchiyama, S.: Giant magnetoresistance with low saturation field in Ni 14 Fe 13 Co 73 / Cu multilayers. Jpn. J. Appl. Phys. **33**, L850 (1994)
23. Oppeneer, P.M., Antonov, V.N., Yaresko, A.N., Perlov, A.Ya., Kraft, T., Eschrig, H.: First-principles theory and predictions of the Kerr effect. J. Magn. Soc. Jpn **20**, S147 (1996)
24. Ma, J., Hegde, V.I., Munira, K., Xie, Y., Keshavarz, S., Mildebrath, D.T., Wolverton, C., Ghosh, A.W., Butler, W.H.: Computational

investigation of half-Heusler compounds for spintronics applications. Phys. Rev. B **95**, 024411 (2017)
25. Blaha, P., Schwarz, K., Madsen, G.K.H., Kvasnicka, D., Luitz, J.: WIEN2K, An Augmented Plane Wave + Local Orbitals Program for Calculating Crystal Properties, Karlheinz Schwarz, Techn. Universität Wien, Austria, Wien, Austria (2001)
26. Singh, D.J., Nordström, L.: Planewaves, Pseudopotentials, and the LAPW Method. Springer, New York (2006)
27. Perdew, J.P., Chevary, J.A., Vosko, S.H., Jackson, K.A., Pederson, M.R., Singh, D., Fiolhais, C.: Atoms, molecules, solids, and surfaces: Applications of the generalized gradient approximation for exchange and correlation. Phys. Rev. B **46**, 6671 (1992)
28. Perdew, J.P., Burke, K., Ernzerhof, M.: Generalized gradient approximation made simple. Phys. Rev. Lett. **77**, 3865 (1996)
29. Barth, U.V., Hedin, L.: A local exchange-correlation potential for the spin polarized case. i. J. Phys. C Solid State Phys. **5**, 1629 (1972)
30. Pant, M.M., Rajagopal, A.K.: Theory of inhomogeneous magnetic electron gas. Solid State Commun. **10**, 1157 (1972)
31. Galankis, I., Dederiches, P.H.: Half-Metallic Alloys: Fundamentals and Applications. Springer, Berlin (2005)
32. Galanakis, I., Dederichs, P.H., Papanikolaou, N.: SLater-Pauling behavior and origin of the half-metallicity of the full-Heusler alloys. Phys. Rev. B **66**, 174429 (2002)
33. Fox, A.M.: Optical Properties of Solids. Oxford University Press, New York (2001)
34. Wooten, F.: Optical Properties of Solids. Academic Press, New York (1972)